OPEN

Citation: Transl Psychiatry (2014) 4, e417; doi:10.1038/tp.2014.59

www.nature.com/tp

ORIGINAL ARTICLE

Free D-aspartate regulates neuronal dendritic morphology, synaptic plasticity, gray matter volume and brain activity in mammals

F Errico[1,2,13], R Nisticò[3,4,13], A Di Giorgio[5,13], M Squillace[1], D Vitucci[1,6], A Galbusera[7], S Piccinin[8], D Mango[3], L Fazio[9], S Middei[3], S Trizio[9], NB Mercuri[3,10], MA Teule[3], D Centonze[3,10], A Gozzi[7], G Blasi[9], A Bertolino[9,11,14] and A Usiello[1,12,14]

D-aspartate (D-Asp) is an atypical amino acid, which is especially abundant in the developing mammalian brain, and can bind to and activate N-methyl-D-Aspartate receptors (NMDARs). In line with its pharmacological features, we find that mice chronically treated with D-Asp show enhanced NMDAR-mediated miniature excitatory postsynaptic currents and basal cerebral blood volume in fronto-hippocampal areas. In addition, we show that both chronic administration of D-Asp and deletion of the gene coding for the catabolic enzyme D-aspartate oxidase (DDO) trigger plastic modifications of neuronal cytoarchitecture in the prefrontal cortex and CA1 subfield of the hippocampus and promote a cytochalasin D-sensitive form of synaptic plasticity in adult mouse brains. To translate these findings in humans and consistent with the experiments using *Ddo* gene targeting in animals, we performed a hierarchical stepwise translational genetic approach. Specifically, we investigated the association of variation in the gene coding for DDO with complex human prefrontal phenotypes. We demonstrate that genetic variation predicting reduced expression of *DDO* in postmortem human prefrontal cortex is mapped on greater prefrontal gray matter and activity during working memory as measured with MRI. In conclusion our results identify novel NMDAR-dependent effects of D-Asp on plasticity and physiology in rodents, which also map to prefrontal phenotypes in humans.

Translational Psychiatry (2014) **4,** e417; doi:10.1038/tp.2014.59; published online 29 July 2014

INTRODUCTION

Recent evidence supports a role for D-amino acids as a novel class of neuromodulators.[1,2] It is well established that D-serine (D-Ser) acts as a 'gliotransmitter' that modulates N-Methyl-D-Aspartate receptor (NMDAR) transmission and, in turn, affects several physiological processes,[3–6] including dendritic morphology, synaptic plasticity and cognition.[7–10] On the other hand, dysregulation of D-Ser metabolism has been observed in neuropsychiatric disorders such as schizophrenia.[11–13] Differently from D-Ser, the biological role of the other D-amino acid consistently found in the mammalian brain, D-aspartate (D-Asp), has been so far less characterized. D-Asp occurs at high levels during embryonic stages and strongly decreases after birth, due to the concomitant expression of the catabolic enzyme D-aspartate oxidase (DDO).[14] Pharmacological studies reported that D-Asp activates NMDARs by binding to the glutamate site on GluN2 subunits.[15] In support of a role for D-Asp on NMDAR-mediated transmission, it has been shown that higher levels of D-Asp increased hippocampal NMDAR-dependent early phase of long-term potentiation (E-LTP)[15–17] and spatial memory[15,17,18] in knockout mice for *Ddo* gene ($Ddo^{-/-}$) and in D-Asp-treated mice. On the other side, short-hairpin RNA-mediated depletion of the enzyme involved in the biosynthesis of D-Asp, aspartate racemase (DR), triggers substantial defects in dendritic arborization and survival of newborn neurons in the adult hippocampus.[19] Finally, neurochemical observations evidenced that D-Asp levels are reduced in the postmortem prefrontal cortex (PFC) of patients with schizophrenia,[20] a disorder in which dysregulation of glutamate in PFC is centrally implicated.[21,22]

On the basis of the common pharmacological ability of D-Ser and D-Asp to activate NMDAR-dependent transmission, we hypothesized that D-Asp, like D-Ser, affects structural and functional neuroplasticity in the adult mammalian brain. To this aim, as D-Asp levels are low in adulthood, we employed mice with forcedly higher levels of D-Asp, produced either by 1-month oral administration of this D-amino acid or by targeted deletion of the *Ddo* gene. Moreover, in an effort to translate these pharmacological and genetic manipulations in rodents to humans, we used a hierarchical stepwise translational genetic approach to investigate

[1]Laboratory of Behavioural Neuroscience, Ceinge Biotecnologie Avanzate, Naples, Italy; [2]Department of Molecular Medicine and Medical Biotechnology, University of Naples 'Federico II', Naples, Italy; [3]Centro Europeo per la Ricerca sul Cervello (CERC)/Fondazione Santa Lucia, Rome, Italy; [4]Department of Physiology and Pharmacology, Sapienza University of Rome, Rome, Italy; [5]Istituto di Ricovero e Cura a Carattere Scientifico 'Casa Sollievo della Sofferenza', San Giovanni Rotondo, Italy; [6]Faculty of Motor Sciences, University of Naples 'Parthenope', Naples, Italy; [7]Istituto Italiano di Tecnologia, Center for Neuroscience and Cognitive Systems, Rovereto, Italy; [8]Pharmacology of Synaptic Plasticity Unit, European Brain Research Institute (EBRI), Rome, Italy; [9]Group of Psychiatric Neuroscience, Department of Neuroscience, Basic Sciences and Sense Organs, University of Bari 'Aldo Moro', Bari, Italy; [10]Department of Neuroscience, Tor Vergata University Hospital Foundation, Rome, Italy; [11]pRED, Neuroscience DTA, Hoffman-La Roche, Ltd, Basel, Switzerland and [12]Department of Environmental, Biological and Pharmaceutical Sciences and Technologies, Second University of Naples (SUN), Caserta, Italy. Correspondence: Professor A Bertolino, Group of Psychiatric Neuroscience, Department of Neuroscience, Basic Sciences and Sense Organs, University of Bari 'Aldo Moro', 70121 Bari, Italy or Professor A Usiello, Laboratory of Behavioural Neuroscience, Ceinge Biotecnologie Avanzate, Via G. Salvatore, 486, 80145 Naples, Italy.
E-mail: alessandro.bertolino@uniba.it or usiello@ceinge.unina.it
[13]Share co-first authorship.
[14]Share co-last authorship.
Received 27 November 2013; revised 25 April 2014; accepted 4 June 2014

whether genetic variation of the *DDO* gene (6q21) affects *DDO* mRNA expression and, in turn, modulates prefrontal gray matter volume and activity during working memory (WM) processing in healthy subjects.

MATERIALS AND METHODS

Animals

C57BL/6J male mice were used to test the effects of 1-month-long oral administration of D-Asp. D-Asp was delivered in drinking water at the concentration of 20 mM to 3-month-old mice until the age of 4 months, when they were used for experiments. Mutant mice for the *Ddo* gene were generated and genotyped by PCR as described previously.[23] All research involving animals was carried out in accordance with the European directive 86/609/EEC governing animal welfare and protection, which is acknowledged by the Italian Legislative Decree no. 116, 27 January 1992. Animal research protocols were also reviewed and consented to by a local animal care committee.

Electrophysiology

Coronal slices from mouse medial PFC (mPFC; 250 μm) were cut in ice-cold artificial cerebrospinal fluid using standard procedures. Visually guided whole-cell recordings were performed as previously described[24] (see also Supplementary Methods) using 1.5 mm borosilicate glass electrodes (3–4 MΩ) filled with a solution containing (in mM) $CsMeSO_4$ (130), HEPES (5.0), EGTA (0.5), $MgCl_2$ (1.0), NaCl (1.0), $CaCl_2$ (0.34), QX-314 (5.0), adjusted to pH 7.3 with CsOH. Miniature excitatory postsynaptic currents (mEPSCs) were collected from layer II/III mPFC pyramidal neurons and NMDA currents were pharmacologically isolated according to a previously described procedure.[25]

For extracellular recordings, parasagittal hippocampal slices (thickness, 400 μm) were cut using a Vibratome (Leica VT1000 S, Leica Biosystems, Wetzlar, Germany). Slices were incubated for 1 h in a holding chamber and then transferred to a recording chamber, completely submerged in artificial cerebrospinal fluid (30–31 °C) of the following composition (in mM): NaCl (124), KCl (3.0), $MgCl_2$ (1.0), $CaCl_2$ (2.0), NaH_2PO_4 (1.25), $NaHCO_3$ (26), glucose (10); saturated with 95% O_2, 5% CO_2. Bipolar stimulating electrodes placed in the stratum radiatum to activate the Schaffer collateral commissural fibers. Recordings of field excitatory postsynaptic potentials were made in the middle of the stratum radiatum by using microelectrodes filled with artificial cerebrospinal fluid (resistance 3–5 MΩ). LTP was induced with 1 s, 100 Hz stimulation. For statistical analysis we used unpaired *t*-tests after LTP induction (on the average of the last 10 min of recording).

Functional magnetic resonance imaging measurement of basal cerebral blood volume

Animal preparation for functional magnetic resonance imaging (fMRI) was adapted from previous studies[26–28] and optimized for physiological stability. Briefly, mice were anesthetized with halothane, intubated and artificially ventilated. A femoral artery was cannulated for contrast agent administration, blood pressure monitoring and sampling, and infusion of paralyzing agent. Experiments were carried out at a maintenance anesthesia level of 0.7%. Ventilation parameters were adjusted to maintain physiological levels of arterial blood gases ($paCO_2$ and paO_2). Image acquisition parameters have been recently described.[29] High-resolution anatomical images were acquired at 7 Tesla with a fast spin echo sequence. Co-centered cerebral blood volume (CBV) weighted fMRI times series were acquired using a fast low-angle shot sequence with a TR = 394.7 ms, TE = 3.1 ms, α = 30°; FOV 2 × 2 cm^2, 156 × 156 × 500 μm resolution, dt = 60 s. Images were sensitized to reflect alterations in CBV[30–32] by injecting 5 μl g^{-1} of superparamagnetic iron oxide (Molday Ion, Biopal Inc., Worcester, MA, USA) intraarterially after five baseline images. The procedure used to calculate basal CBV (bCBV) has been recently described in greater detail.[29,33] bCBV time-series were calculated over a 5-min time-window starting 15 min after contrast agent injection and spatially normalized to a study-based anatomical template. Voxel-wise group statistics was carried out using FSL using multilevel Bayesian inference and a *Z*-threshold > 1.7, a corrected cluster significance threshold of $P = 0.001$.[34] Age, weight and terminal arterial gas levels ($paCO_2$) were used as nuisance regressors in the design matrix.

Golgi-Cox staining and dendritic spine measurements

Golgi-Cox staining was performed on brains of naive animals, according to a previous protocol.[35] Fully impregnated pyramidal neurons laying in the PFC and in the CA1 region of the dorsal hippocampus were visualized at ×100 (oil-immersion) using a microscope (DMLB, Leica Biosystems) equipped with a camera (resolution = 2600 × 2600, Axiocam, Zeiss AG, Oberkochen, Germany), and the KS300 3.0 system (Zeiss). A computer-based neuron tracing system (Neurolucida, Microbrightfield, MBF Bioscience, Williston, VT, USA) was used to trace single neurons. Total dendritic length and spine density were calculated according to D'Amelio *et al.*[35] and analyzed using Student's *t*-test. Dendritic complexity was calculated according to Balu *et al.*[7] and analyzed using two-way analysis of variance with repeated measures, followed by Fisher's *post hoc* comparison when required.

Candidate *DDO* SNPs screening and mRNA expression

Data from 268 brains of nonpsychiatric individuals (176 males; mean age ± s.d. 27.89 ± 22.15 years; pH 6.53 ± 0.3; postmortem interval: 26.37 ± 17.11) were analyzed (Supplementary Table 1). These data were obtained from the largest postmortem collection publicly available (BRAINCLOUD, courtesy of the Lieber Institute for Brain Development, Baltimore, USA[36] (http://braincloud.jhmi.edu)). Details of tissue acquisition, handling, processing, dissection, clinical characterization, diagnoses, neuropathological examinations, RNA extraction and quality control measures were described previously.[36] From each subject in the brain collection, RNA from prefrontal gray matter was analyzed using spotted oligonucleotide microarrays yielding data from 30 176 gene expression probes and allowing us to focus on *DDO* mRNA expression (see Supplementary Information). After normalization,[37] log_2 intensity ratios were further adjusted to reduce the impact of known and unknown sources of systematic noise on gene expression measures using surrogate variable analysis.[38] DNA from cerebellar tissue was studied with Illumina (Illumina Inc., San Diego, CA, USA) BeadChips producing 625 439 SNP genotypes called using the BeadExpress software for each subject as described elsewhere[36] (see also Supplementary Methods). For the purpose of this study, we selected *DDO* mRNA expression in prefrontal cortex and all SNPs ($n = 92$) within *DDO*. Two of these SNPs (rs2057149 and rs3757351) were significantly associated with *DDO* mRNA expression (see results section) and were thus used for *in vivo* analysis with imaging tools (see below).

Imaging

All subjects participating in the imaging protocols were Caucasian healthy volunteers matched for age, gender or IQ across *DDO* genotype groups (Supplementary Table 2 and Table 3). All SNP associations were tested in Statistical Parametric Mapping 8.0 (http://www.fil.ion.ucl.ac.uk/spm) with random effects analyses. For gray matter volumes ($n = 152$), we performed voxel-based morphometry (VBM) following standardized methods (new segmentation and diffeomorphic registration algorithms) with appropriate covariates as described previously[39] (Supplementary Methods). During 3T BOLD fMRI scanning, subjects ($n = 143$) performed a WM task (1- and 2-back) to robustly engage the dorsolateral PFC as in previous reports[40] (Supplementary Methods). Random-effects analyses were performed on *a priori* defined regions of interest with genotype as predictor and load as the repeated measures factor. Statistical correction for multiple comparisons within the regions of interest was performed as appropriate, respectively, for VBM and fMRI data (Supplementary Methods).

RESULTS

Oral administration of D-Asp affects NMDAR-mediated miniature excitatory postsynaptic currents and basal metabolic function in fronto-hippocampal areas of adult mice

We first measured the ability of exogenous application of D-Asp to modulate isolated NMDAR currents from mPFC layer II/III pyramidal neurons, a cortical layer implicated in schizophrenia-like phenotypes in mice.[25] Data obtained in C57BL/6J mice show that perfusion of D-Asp (300 μM) on mPFC slices did not affect the cumulative distribution of NMDAR components of miniature excitatory postsynaptic currents ($mEPSC_{NMDA}$) amplitude ($P > 0.05$; Figure 1a, left panel), but reduced the inter-event

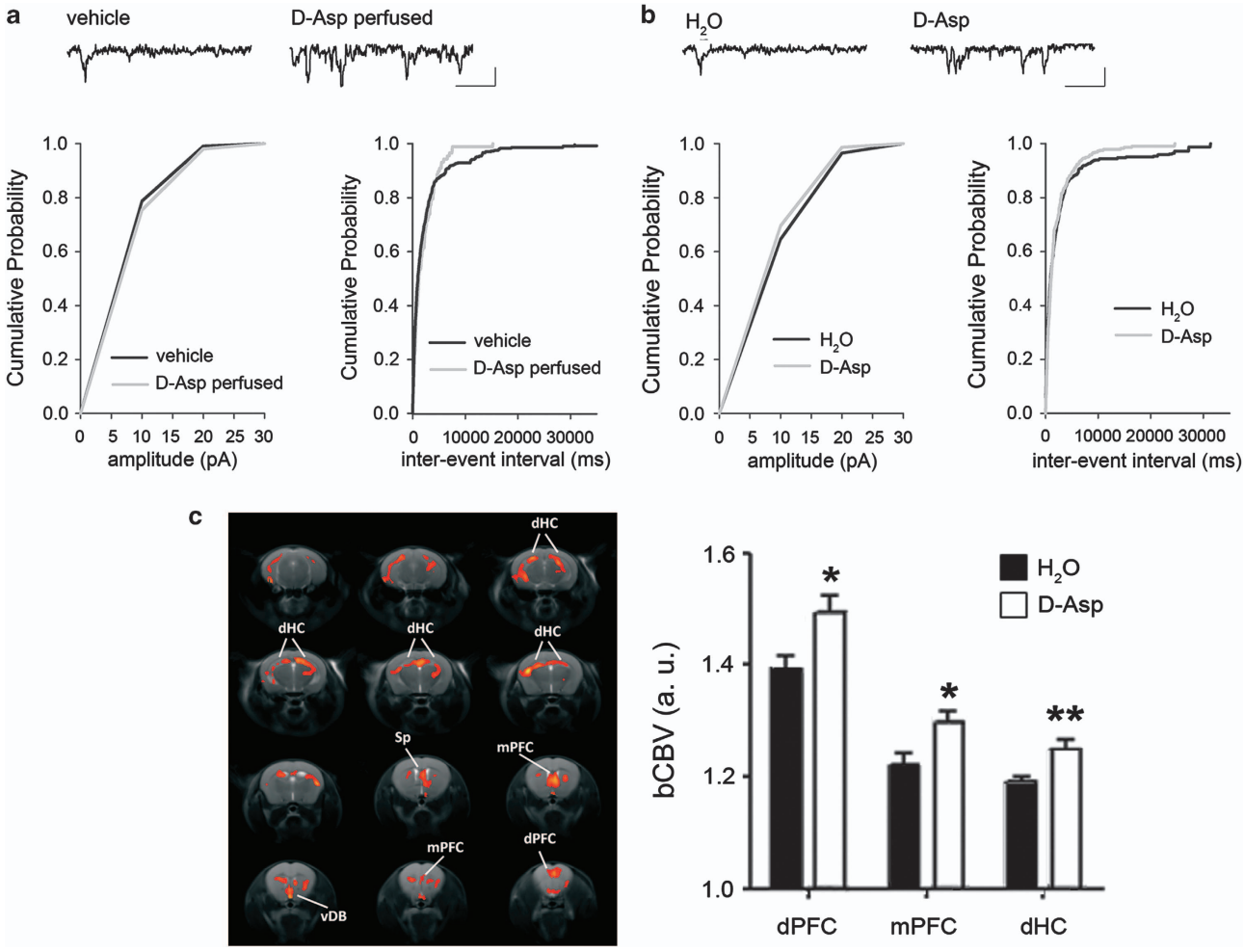

Figure 1. Effect of D-aspartate (D-Asp) treatment on NMDAR-dependent miniature excitatory post-synaptic currents and basal metabolic function in fronto-septo-hippocampal areas of adult mice. (**a**) Pooled (mean) cumulative distributions of $mEPSCs_{NMDA}$ amplitude (left panel, $n=8$ for vehicle, $n=8$ for D-Asp perfused; bin size 10 pA; K-S test $P>0.05$) and inter-event interval (right panel, $n=8$ for vehicle, $n=8$ for D-Asp perfused; bin size 50 ms; K-S test $P<0.001$) recorded in mPFC layer II/III pyramidal neurons in the absence or presence of perfused D-Asp (300 μM). Representative traces of NMDAR current detected in the mPFC layer II/III pyramidal neurons before and after exogenous perfusion of D-Asp (top). Scale: vertical bar, 10 pA; horizontal bar, 1s. (**b**) Pooled (mean) cumulative distributions of $mEPSCs_{NMDA}$ amplitude (left panel, $n=9$ for H_2O, $n=9$ for D-Asp; bin size 50 ms; K-S test $P>0.05$) and inter-event interval (right panel, $n=9$ for H_2O, $n=9$ for D-Asp; bin size 50 ms; K-S test $P<0.001$) recorded in the mPFC layer II/III pyramidal neurons from C57BL/6J mice untreated or treated for 1 month with a 20 mM D-Asp solution. (**c**) Anatomical distribution of brain areas exhibiting a significant increase in bCBV in mice exposed to D-Asp with respect to vehicle controls ($P<1.7$, corrected cluster significance $P=0.001$). Activation maps (red/orange) are superimposed onto contiguous 0.75 mm MRI coronal images. a.u., arbitrary unit; DdHC, dorsal hippocampus; dPFC, dorsal prefrontal cortex; mPFC, medial prefrontal cortex; Sp, septum; vDB, ventral diagonal band.

interval of $mEPSC_{NMDA}$, as observed by the leftward shift of the cumulative mEPSCs inter-event interval distribution compared with control ($P<0.001$; Figure 1a, right panel). A complete dose–response curve on the effects of D-Asp on $mEPSC_{NMDA}$ is shown in Supplementary Figure 1. We then assessed in mice the effects of chronic treatment (1 month) with 20 mM D-Asp, an administration schedule known to substantially increase the levels of this D-amino acid in the mouse brain (about 2–5-fold).[18,41] Similar to what was observed following exogenous application, chronic treatment with D-Asp to animals did not affect the cumulative distributions of $mEPSC_{NMDA}$ amplitude ($P>0.05$; Figure 1b, left panel) but induced a significant leftward shift of the cumulative inter-event interval distribution of neurons compared with control ($P<0.001$; Figure 1b, right panel). Next, we investigated the possible effects of greater D-Asp-induced NMDAR-mediated transmission on basal cerebral metabolism as assessed with bCBV-weighted fMRI, a well-established marker of resting neuronal activity and metabolism in rodents.[30,33,42]

Interestingly, voxel-wise bCBV mapping revealed region-specific foci of significantly greater bCBV in D-Asp-treated animals as compared with controls ($Z>1.6$, corrected cluster significance, $P<0.001$) that encompassed several fronto-septo-hippocampal regions, including the dorsal and mPFC, septum and dorsal hippocampus (Figure 1c). The effect was statistically significant also when expressed in terms of mean activation over predefined anatomical volume of interests ($P<0.05$, all regions, Student's *t*-test; Figure 1c). No brain regions exhibited significant reductions of bCBV in D-Asp-treated animals. No significant differences in arterial pCO_2 (or pO_2) levels were observed between groups at the end of the fMRI sessions ($P>0.88$, Student's *t*-test), thus allowing to rule out a contribution of unspecific vasoactive events to the differences mapped.

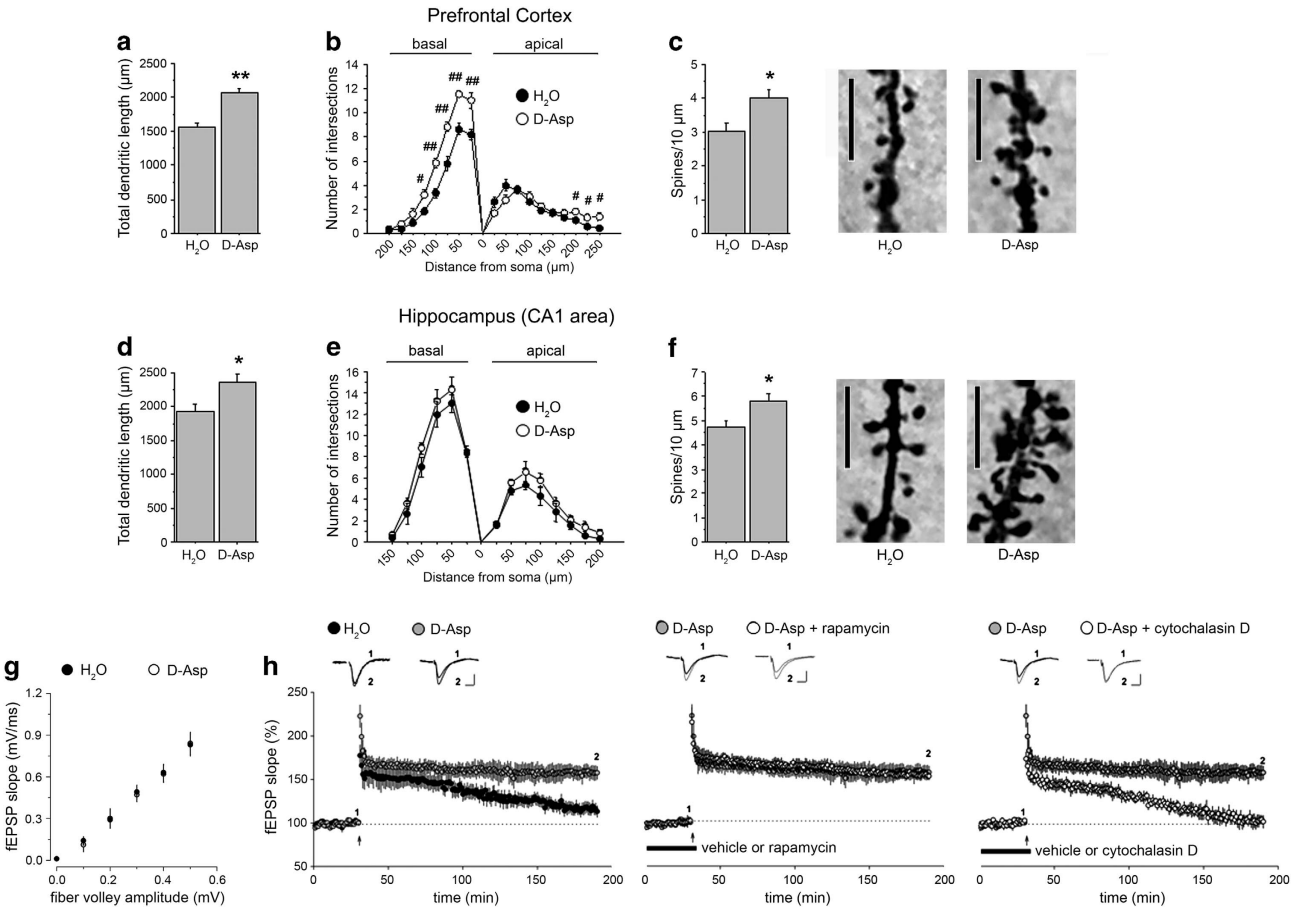

Figure 2. Dendritic morphology and late-phase LTP in mice treated with D-aspartate (D-Asp). Analysis of dendritic morphology was performed on C57BL/6J mice drinking D-Asp or H_2O in pyramidal neurons of the (**a–c**) PFC ($n = 5$ mice per treatment, 5 neurons per mouse) and (**d–f**) CA1 subfield of the hippocampus ($n = 5$ mice per treatment, 4 neurons per mouse) after Golgi-Cox staining. (**a** and **d**) Total dendritic length (in µm) measured in the (**a**) PFC and (**d**) CA1 subfield of the hippocampus. (**b** and **e**) Number of intersections between basal or apical dendrites and Sholl concentric circle lines at different distances from soma center in both (**b**) PFC and (**e**) CA1 area. Concentric circles increase in diameter by 25 µm increments. (**c** and **f**) Spine density (number of spines per 10 µm) evaluated in (**c**) the PFC and (**f**) CA1 area of mice. The right panels show representative dendrites. $^{**}P < 0.01$, $^{*}P < 0.05$, compared with untreated mice (Student's *t*-test). $^{\#\#}P < 0.01$, $^{\#}P < 0.05$, compared with untreated mice (Fisher's *post hoc*). Scale bar, 5 µm. (**g**) Input–output relation of field excitatory postsynaptic potentials (fEPSPs) as a function of presynaptic fiber volley size shows similar fEPSPs slopes over a range of stimulus intensities for both untreated C57BL/6J ($n = 6$) and D-Asp-treated C57BL/6J ($n = 6$) mice. Data are expressed as mean ± s.e.m. ($P > 0.05$, Student's *t*-test). (**h**) Time plot of hippocampal fEPSP responses showing the effect of E-LTP stimulation paradigm in untreated C57BL/6J mice and D-Asp-treated C57BL/6J mice ($n = 6$ mice per treatment; left panel). Hippocampal L-LTP in D-Asp-treated mice was unaffected following bath-application of 20 nM rapamycin (transiently bath-applied for 40 min; $n = 6$ vehicle-treated slices, $n = 5$ rapamycin-treated slices; middle graph) but was fully blocked following bath-application of 100 nM cytochalasin D (continuously bath-applied; $n = 6$ vehicle-treated slices, $n = 5$ cytochalasin D-treated slices; right panel). Insets show field EPSPs from representative experiments during baseline and following LTP induction (1 s, 100 Hz tetanus). Vertical bar, 0.5 mV; horizontal bar, 10 ms. LTP, long-term potentiation; PFC, prefrontal cortex.

Oral administration of D-Asp in adult mice influences neuronal spine density, dendritic length and converts E-LTP into L-LTP in the hippocampus

To investigate the possible structural changes associated with increased NMDAR-dependent transmission, a Golgi-Cox analysis was performed in adult D-Asp-treated mice in the same brain regions where we observed increased bCBV. Consistent with neuroimaging, pyramidal neurons of the PFC exhibited significantly increased dendritic length in D-Asp-treated mice, compared with the untreated group (H_2O vs D-Asp (mean ± s.e.m.): 1564.33 ± 62.16 µm vs 2068.94 ± 49.13 µm, $P < 0.01$; Figure 2a). Moreover, count of dendritic intersections by Sholl analysis revealed different arborization of basal dendritic segments between D-Asp-treated mice and controls (treatment: $F_{(1,56)} = 55.438$, $P < 0.0001$; distance from soma x treatment: $F_{(7,56)} = 6.019$, $P < 0001$; Figure 2b). More in detail, the complexity of dendritic tree in D-Asp-treated group is greater between 25 and 125 µm ($P < 0.01$ at 25, 50, 75 and 100 µm; $P < 0.05$ at 125 µm). The apical dendritic complexity is also different between treatments (distance from soma × genotype: $F_{(9,72)} = 5.111$, $P < 0.0001$; Figure 2b). In particular, increased number of dendritic segments appears between 200 and 250 µm in animals drinking D-Asp ($P < 0.05$). Finally, oral administration of D-Asp is also associated with increased spine density in prefrontal cortical neurons (H_2O vs D-Asp (mean ± s.e.m.): 3.03 ± 0.25 spines per 10 µm vs 4.01 ± 0.25 spines per 10 µm, $P < 0.05$; Figure 2c).

Next, we examined dendritic architecture of pyramidal neurons in the CA1 area of the hippocampus. Morphological analysis revealed a similar trophic effect for D-Asp in this area. More specifically, we found a significant extension of dendrites in animals treated with D-Asp, compared with controls (H_2O vs D-Asp (mean ± s.e.m.): 1925.80 ± 98.97 µm vs 2352.93 ± 126.97 µm,

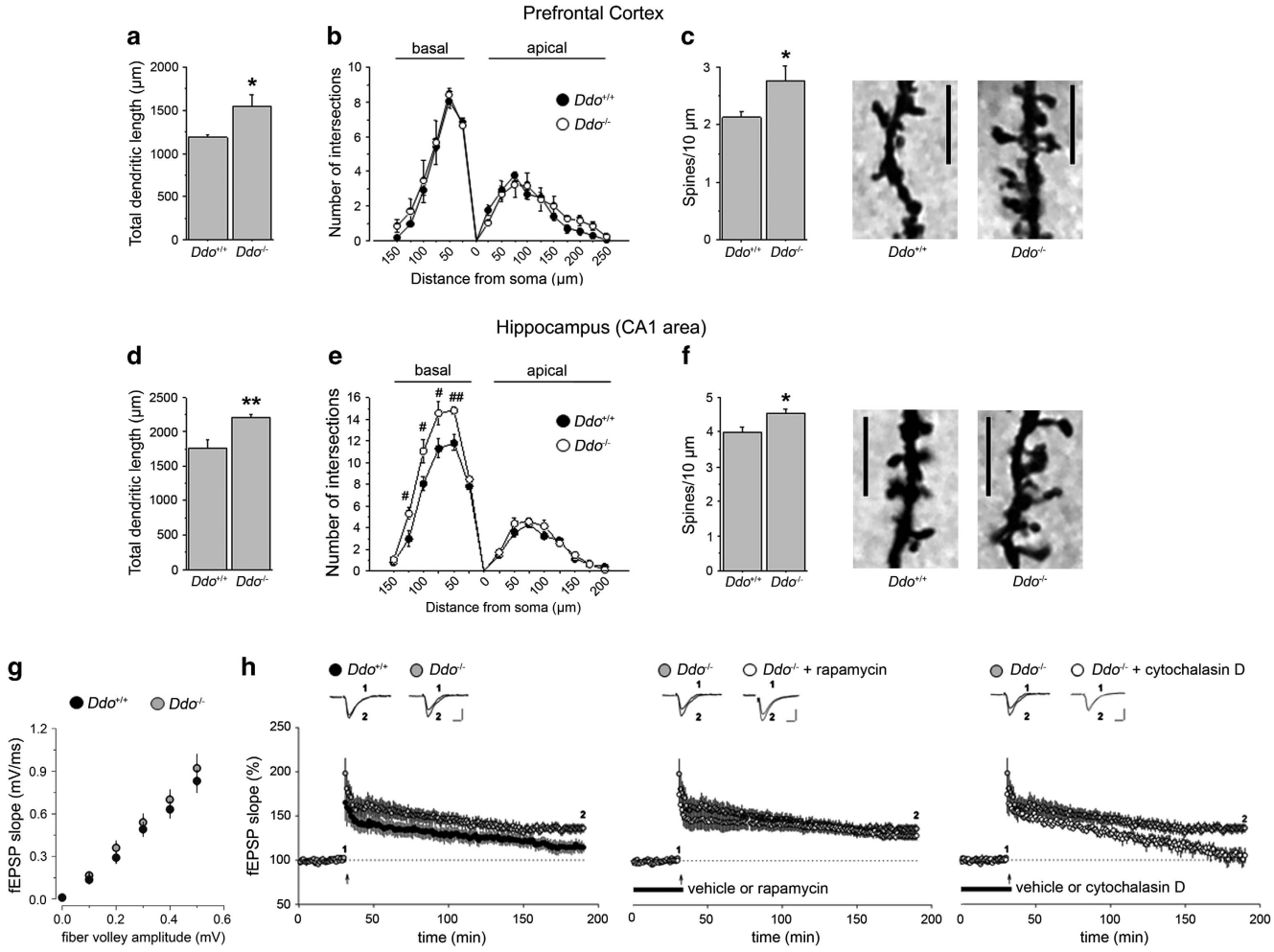

Figure 3. Dendritic morphology and late-phase LTP in $Ddo^{-/-}$ mice. Analysis of dendritic morphology was performed on $Ddo^{+/+}$ and $Ddo^{-/-}$ mice in pyramidal neurons of the (**a–c**) PFC ($n = 5$ mice per genotype, 3 neurons per mouse) and (**d–f**) CA1 subfield of the hippocampus ($n = 5$ mice per genotype, 4 neurons per mouse) after Golgi-Cox staining. (**a** and **d**) Total dendritic length (in µm) performed in the (**a**) PFC and (**d**) CA1 subfield of the hippocampus. (**b** and **e**) Number of intersections between basal or apical dendrites and Sholl concentric circle lines at different distances from soma center in both (**b**) PFC and (**e**) CA1 area. Concentric circles increase in diameter by 25 µm increments. (**c** and **f**) Spine density (number of spines per 10 µm) evaluated in both (**c**) the PFC and (**f**) the CA1 area. The right panels show representative dendrites. $^{*}P < 0.05$, compared with $Ddo^{+/+}$ mice (Student's *t*-test). $^{\#\#}P < 0.01$, $^{\#}P < 0.05$, compared with $Ddo^{+/+}$ mice (Fisher's *post hoc*). Scale bar, 5 µm. (**g**) Input–output relation shows comparable fEPSPs slopes for both $Ddo^{+/+}$ ($n = 6$) and $Ddo^{-/-}$ ($n = 6$) littermates ($P > 0.05$, Student's *t*-test). (**h**) Time plot of hippocampal fEPSP responses showing that (left panel) an E-LTP stimulation paradigm elicited E-LTP in $Ddo^{+/+}$ mice and L-LTP in $Ddo^{-/-}$ mice ($n = 7$ for $Ddo^{+/+}$, $n = 7$ for $Ddo^{-/-}$; left panel). Hippocampal L-LTP in $Ddo^{-/-}$ slices was insensitive to the effects of rapamycin (transiently bath-applied for 40 min; $n = 7$ vehicle-treated $Ddo^{-/-}$ slices, $n = 5$ rapamycin-treated $Ddo^{-/-}$ slices; middle panel) but was fully prevented by cytochalasin D (continuously bath-applied; $n = 7$ for vehicle-treated $Ddo^{-/-}$ slices, $n = 6$ for cytochalasin D-treated $Ddo^{-/-}$ slices; right panel). Insets show field EPSPs from representative experiments during a baseline interval and following LTP induction (1 s, 100 Hz tetanus). Scale: vertical bar, 0.5 mV; horizontal bar, 10 ms. All data are expressed as mean ± s.e.m. LTP, long-term potentiation; PFC, prefrontal cortex.

$P < 0.05$; Figure 2d). Complexity of basal and apical dendrites is similar between treatments (Figure 2e). Density of spines is also increased in D-Asp-treated mice, compared with untreated animals (H_2O vs D-Asp (mean ± s.e.m.): 4.74 ± 0.25 spines per 10 µm vs 5.78 ± 0.33 spines per 10 µm, $P < 0.05$; Figure 2f). For further morphological analyses, see Supplementary Results and Supplementary Figure 2.

Dendritic spine density and morphology are strictly correlated with functional synaptic plasticity.[43,44] Based on dendritic structural modifications associated with oral D-Asp administration, we investigated baseline synaptic transmission and LTP at hippocampal CA1 synapses of D-Asp-treated animals. No significant differences in stimulus-response curves were observed between D-Asp-treated mice and control mice ($P > 0.05$; Figure 2g). Next, we used an early-LTP (E-LTP) induction paradigm (100 Hz, 1 s) and recorded responses for 3 h. As expected, this paradigm caused decaying LTP in wild-type slices after 1 h but, strikingly, it was sufficient to induce stable L-LTP in D-Asp-treated mice (LTP at 160 min, $H_2O = 16 \pm 7\%$; D-Asp = 57 ± 7%; *t*-test, last 10 min of recording, $P < 0.001$; Figure 2h, left panel). As this long-lasting form of LTP has been reported to be sensitive to rapamycin,[45,46] we tested whether the lowered threshold for the induction of L-LTP following D-Asp oral administration could be influenced by this compound. Notably, when rapamycin was administered before the conditioning train, L-LTP still persisted (LTP at 160 min, vehicle = 57 ± 7%, rapamycin = 53 ± 4%; *t*-test, last 10 min of recording, $P > 0.05$; Figure 2h, middle panel). On the other hand, also rearrangements of cytoskeleton have been recently found to be crucial in L-LTP.[47] Therefore, we tested the effect of the actin polymerization inhibitor, cytochalasin D. Remarkably, L-LTP was fully prevented in D-Asp-treated mice in the presence of this drug (LTP at 160 min, vehicle = 57 ± 7%,

cytochalasin D = 4 ± 5%; *t*-test, last 10 min of recording, $P < 0.001$; Figure 2h, right panel).

Genetic inactivation of *Ddo* gene in mice affects spine density, dendritic length and converts E-LTP into L-LTP in the adult hippocampus

To further evaluate the influence of deregulated high levels of D-Asp on structural and functional synaptic plasticity, we also used knockout mice for *Ddo* gene, that show a 10–20-fold increase in the cerebral content of D-Asp.[41] In the PFC, total dendritic length of pyramidal neurons was significantly increased in $Ddo^{-/-}$ mice, compared with controls ($Ddo^{+/+}$ vs $Ddo^{-/-}$ (mean ± s.e.m.): 1189.37 ± 28.63 μm vs 1537.47 ± 138.10 μm, $P < 0.05$; Figure 3a). Sholl analysis revealed no difference in the complexity of basal and apical dendrites between $Ddo^{+/+}$ and $Ddo^{-/-}$ mice (Figure 3b). Conversely, dendrites from $Ddo^{-/-}$ pyramidal neurons have greater spine density compared with control neurons ($Ddo^{+/+}$ vs $Ddo^{-/-}$ (mean ± s.e.m.): 2.12 ± 0.09 spines per 10 μm vs 2.76 ± 0.24 spines per 10 μm, $P < 0.05$; Figure 3c). We then examined dendritic architecture of pyramidal neurons in the CA1 area of the hippocampus. Dendritic length was significantly increased in $Ddo^{-/-}$ mice, compared with $Ddo^{+/+}$ animals ($Ddo^{+/+}$ vs $Ddo^{-/-}$ (mean ± s.e.m.): 1765.25 ± 117.58 μm vs 2219.51 ± 43.86 μm, $P < 0.01$; Figure 3d). Sholl analysis revealed a significantly different morphological organization of basal dendrites between genotypes (genotype: $F_{(1,40)} = 8.131$, $P = 0.0214$; distance from soma × genotype: $F_{(5,40)} = 4.152$, $P = 0.0039$; Figure 3e), as revealed by a greater number of intersections in $Ddo^{-/-}$ mice between 50 and 125 μm, compared with controls ($P < 0.01$ at 50 μm; $P < 0.05$ at 75, 100 and 125 μm). Apical intersections are not different between genotypes (Figure 3e). Also, spine density is significantly increased in $Ddo^{-/-}$ mice, compared with controls [$Ddo^{+/+}$ vs $Ddo^{-/-}$ (mean ± s.e.m.):

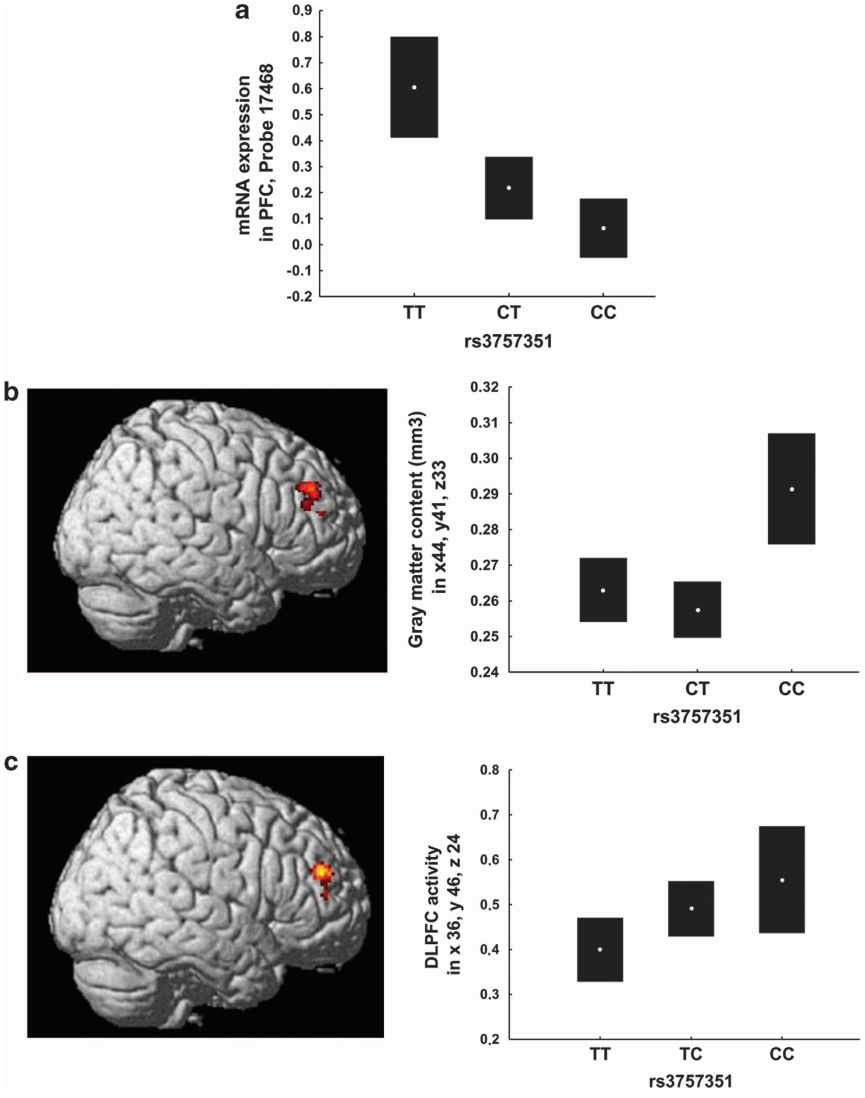

Figure 4. Association of *DDO* rs3757351 with prefrontal phenotypes in humans. (**a**) Association of *DDO* rs3757351 with DDO mRNA expression levels in postmortem PFC ($n = 268$). Graph depicts normalized $\log_2$ ratios (sample/reference). Data from http://braincloud.jhmi.edu/; (**b**) Association of *DDO* rs3757351 with prefrontal gray matter volume in Caucasian healthy subjects ($n = 159$). Left panel: three-dimensional rendering of the prefrontal cluster associated with a main effect of rs3757351. Image thresholded at $P < 0.005$, nonstationary cluster extend corrected. Right panel: graph showing mean ± 0.95 CIs of gray matter content extracted from the cluster depicted in the left panel. (**c**) Association of *DDO* rs3757351 with prefrontal BOLD response during working memory in Caucasian healthy subjects ($n = 143$). Left panel: Three-dimensional rendering of the prefrontal cluster associated with a main effect of rs3757351. Image thresholded at $P < 0.05$, FWE corrected. Right panel: graph showing mean ± 0.95 CIs of parameter estimated extracted from the cluster depicted in the left panel. CI, confidence interval; DLPFC, dorsolateral PFC; PFC, prefrontal cortex.

3.99 ± 0.16 spines per 10 µm vs 4.53 ± 0.13 spines per 10 µm, $P < 0.05$; Figure 3f). For further morphological analyses, see Supplementary Results and Supplementary Figure 3.

Next, we examined whether altered dendritic spine density and length might be associated with changes in synaptic function in $Ddo^{-/-}$ mice. Similar to D-Asp treated mice, no differences were found between the input–output curves of both genotypes ($P > 0.05$; Figure 3g). On the contrary, a single tetanus elicited E-LTP in wild-type slices, whereas it induced a stable L-LTP in $Ddo^{-/-}$ slices (LTP at 160 min, $Ddo^{+/+} = 14 \pm 5\%$, $Ddo^{-/-} = 36 \pm 5\%$; *t*-test, last 10 min of recording, $P < 0.001$; Figure 3h, left panel). This form of L-LTP still persisted in the presence of rapamycin (LTP at 160 min, vehicle = 36 ± 5%, rapamycin = 28 ± 5%; *t*-test, last 10 min of recording, $P > 0.05$; Figure 3h, middle panel), but not of cytochalasin D (LTP at 160 min, vehicle = 36 ± 5%, cytochalasin D = 5 ± 8%; *t*-test, last 10 min of recording, $P < 0.001$; Figure 3h, right panel).

Association of *DDO* genetic variants with human prefrontal *DDO* mRNA expression, prefrontal gray matter volume and physiology during working memory

To investigate the possible translational relevance of these results to humans, we examined the association of variation in the gene coding for the catabolic enzyme DDO with a series of hierarchically more complex prefrontal phenotypes. The phenotype most proximal to genetic variation is mRNA expression. Therefore, we investigated the association of SNPs in the *DDO* gene with mRNA expression in postmortem PFC of healthy human subjects ($n = 268$). Separate analyses of variance on mRNA expression as the dependent variable, and 92 SNPs genotypes as predictors indicate that two intronic SNPs within *DDO* are significantly associated with *DDO* mRNA expression, that is, rs2057149 (A/G) and rs3757351 (C/T) (respectively, $F_{2,265} = 9.6$, $P = 0.01$ and $F_{2,265} = 11.3$, $P = 0.003$, after Bonferroni correction for the number of independent comparisons). In particular, reduced *DDO* mRNA expression is predicted by rs2057149 AA (Fisher's *post hoc* vs AG $P = 0.00005$; vs GG $P = 0.02$) and rs3757351 CC (Fisher's *post hoc* vs CT $P = 0.06$; vs TT $P = 0.000003$; Figure 4a) genotypes.

We further investigated the *in vivo* association of rs2057149 and rs3757351 with prefrontal gray matter volume. Results in healthy humans indicate a main effect of rs3757351 on prefrontal gray matter volume (Montreal Neurological Institute, MNI: x = 44, y = 41, z = 33, $k = 39$, $Z = 3.04$, $P = 0.03$, after nonstationary cluster extent correction; Figure 4b). In particular, CC and CT genotypes predicted greater prefrontal gray matter volume compared with the TT genotype (Fisher's *post hoc,* all $P < 0.005$). rs2057149 was not significantly associated with prefrontal gray matter volume.

Then, we examined the association of rs2057149 and rs3757351 with BOLD fMRI prefrontal activity of healthy humans during performance of the 1- and 2-Back WM task. There was no effect of genotype or genotype by load interaction on behavioral performance (all $P > 0.2$). Thus, the effect of genotype on brain responses during WM processing in this sample reflects how the brain processed WM and not how individuals scored on the task. Imaging results revealed a main effect of rs3757351 on prefrontal activity (MNI: x = 36, y = 46, z = 24, $k = 80$, $Z = 3.35$, $P = 0.04$, after family wise error correction for multiple comparisons, Figure 4c). *Post hoc* analysis on BOLD response extracted from this cluster indicated that subjects with the CC and CT genotypes have greater prefrontal activity when compared with TT individuals (Fisher's *post hoc* $P = 0.02$ and $P = 0.05$, respectively; Figure 4c). No rs3757351 by load interaction was present. Furthermore, no significant association of rs2057149 with prefrontal activity was found.

DISCUSSION

In the present work, we demonstrate that short-term administration of D-Asp, an amino acid enriched in the embryo brain, increases the frequency of NMDAR-mediated mEPSCs in adulthood. The enhancement of NMDAR-dependent transmission in D-Asp-treated mice is mirrored by greater basal metabolic activity, increased dendritic arborization and spine density, and facilitated induction of late-phase LTP. NMDAR signaling is implicated in changes of dendritic spine morphology[48,49] and in induction of persistent forms of plasticity.[50,51] Given the agonistic property of D-Asp on NMDARs, the effects we demonstrate on structural and functional synaptic dynamics in $Ddo^{-/-}$ and D-Asp-treated mice are likely to occur through the activation of NMDARs.

Increased dendritic length and arborization in mice with higher levels of D-Asp is consistent with the severe structural defects in dendritic length and branch number found in the brain of a mouse model with local depletion of D-Asp.[19] Remarkably, in serine racemase-deficient mice, reduction in D-Ser levels that results in NMDAR hypofunction, causes similar morphological defects, as well as alterations in mEPSCs and synaptic plasticity, paralleled by reduced mTOR signaling.[7,8] Based on the evidence that chronic administration of rapamycin produces a comparable reduction of dendritic length and complexity in both $Ddo^{+/+}$ and $Ddo^{-/-}$ mice (see Supplementary Results and Supplementary Figure 4), we cannot rule out that the plastic changes associated to higher D-Asp levels may occur through the activation of mTOR pathway. Previous evidence indicates that storage of long-term memories is likely dependent on enhancement of long-term synaptic plasticity.[52,53] Thus, facilitation of L-LTP induced by higher levels of D-Asp is coherent with the improvement of cognitive abilities previously found in D-Asp-treated and $Ddo^{-/-}$ mice.[15,17,18]

Our results in humans provide further translational validity to these animal models. Variation in the *DDO* gene predicts mRNA levels in prefrontal postmortem tissue, prefrontal gray matter and prefrontal activity during WM processing. More in detail, our findings indicate that the A allele of rs2057149 and the C allele of rs3757351 predict lower DDO mRNA expression relative to rs2057149 G and rs3757351 T alleles, respectively. This association suggests a functional role of these SNPs on modulation of prefrontal DDO levels, which may reflect on D-Asp tone (that is, differential catabolism of D-Asp as a function of *DDO* genetic variation). Consistent with this contention, we found that *DDO* rs3757351 is also associated with *in vivo* prefrontal phenotypes in healthy humans. In particular, our results indicate that the C allele of rs3757351 also predicts greater prefrontal gray matter volume and activity during WM processing relative to the T allele. Thus, genetically mediated reduced expression of *DDO* is mapped on prefrontal phenotypes suggestive of greater prefrontal neuronal plasticity and greater activation of prefrontal neuronal networks during WM.

Previous results have indicated lower levels of D-Asp in the PFC of patients with schizophrenia.[20] Furthermore, converging evidence suggests the possible involvement of NMDAR-dependent signaling in the pathophysiology of this brain disorder,[21,54,55] in which prefrontal dysfunction is crucially implicated.[56] This knowledge and the findings of the present study call for further investigation of the relationship between schizophrenia and D-Asp as well as of the potential relevance of this D-amino acid as a target for treatment of schizophrenia.

CONFLICT OF INTEREST

AB is a full-time employee of Hoffman-La Roche, Ltd. The remaining authors declare no conflict of interest.

ACKNOWLEDGMENTS

We thank F Napolitano, A Di Maio and V Lucignano for their excellent technical support. AU represents the Mariano Scippacercola Foundation. AU was supported by NARSAD Independent Investigator Grant from the Brain & Behavior Research Foundation (Grant no: 20353). FE was supported by grants from the Italian Ministero dell'Istruzione, dell'Università e della Ricerca (FIRB Call—Program 'Futuro in Ricerca 2010'—Project no RBFR10XCD3) and the Italian Ministero della Salute (Call Giovani Ricercatori 2009—Project no GR-2009-1605759).

REFERENCES

1 Mothet JP, Snyder SH. Brain D-amino acids: a novel class of neuromodulators. *Amino Acids* 2012; **43**: 1809–1810.
2 Snyder SH, Ferris CD. Novel neurotransmitters and their neuropsychiatric relevance. *Am J Psychiatry* 2000; **157**: 1738–1751.
3 Fuchs SA, Berger R, de Koning TJ. D-serine: the right or wrong isoform? *Brain Res* 2011; **1401**: 104–117.
4 Billard JM. D: -Amino acids in brain neurotransmission and synaptic plasticity. *Amino Acids* 2012; **43**: 1851–1860.
5 Martineau M, Baux G, Mothet JP. D-serine signalling in the brain: friend and foe. *Trends Neurosci* 2006; **29**: 481–491.
6 Wolosker H, Dumin E, Balan L, Foltyn VN. D-amino acids in the brain: D-serine in neurotransmission and neurodegeneration. *FEBS J* 2008; **275**: 3514–3526.
7 Balu DT, Coyle JT. Neuronal D-serine regulates dendritic architecture in the somatosensory cortex. *Neurosci Lett* 2012; **517**: 77–81.
8 Balu DT, Li Y, Puhl MD, Benneyworth MA, Basu AC, Takagi S *et al.* Multiple risk pathways for schizophrenia converge in serine racemase knockout mice, a mouse model of NMDA receptor hypofunction. *Proc Natl Acad Sci USA* 2013; **110**: E2400–E2409.
9 Bado P, Madeira C, Vargas-Lopes C, Moulin TC, Wasilewska-Sampaio AP, Maretti L *et al.* Effects of low-dose D-serine on recognition and working memory in mice. *Psychopharmacology (Berl)* 2011; **218**: 461–470.
10 Zhang Z, Gong N, Wang W, Xu L, Xu TL. Bell-shaped D-serine actions on hippocampal long-term depression and spatial memory retrieval. *Cereb Cortex* 2008; **18**: 2391–2401.
11 Bendikov I, Nadri C, Amar S, Panizzutti R, De Miranda J, Wolosker H *et al.* A CSF and postmortem brain study of D-serine metabolic parameters in schizophrenia. *Schizophr Res* 2007; **90**: 41–51.
12 Hashimoto K, Engberg G, Shimizu E, Nordin C, Lindstrom LH, Iyo M. Reduced D-serine to total serine ratio in the cerebrospinal fluid of drug naive schizophrenic patients. *Prog Neuropsychopharmacol Biol Psychiatry* 2005; **29**: 767–769.
13 Hashimoto K, Fukushima T, Shimizu E, Komatsu N, Watanabe H, Shinoda N *et al.* Decreased serum levels of D-serine in patients with schizophrenia: evidence in support of the N-methyl-D-aspartate receptor hypofunction hypothesis of schizophrenia. *Arch Gen Psychiatry* 2003; **60**: 572–576.
14 D'Aniello A, Vetere A, Petrucelli L. Further study on the specificity of D-amino acid oxidase and D-aspartate oxidase and time course for complete oxidation of D-amino acids. *Comp Biochem Physiol B* 1993; **105**: 731–734.
15 Errico F, Nistico R, Napolitano F, Mazzola C, Astone D, Pisapia T *et al.* Increased D-aspartate brain content rescues hippocampal age-related synaptic plasticity deterioration of mice. *Neurobiol Aging* 2011; **32**: 2229–2243.
16 Errico F, Nistico R, Palma G, Federici M, Affuso A, Brilli E *et al.* Increased levels of d-aspartate in the hippocampus enhance LTP but do not facilitate cognitive flexibility. *Mol Cell Neurosci* 2008; **37**: 236–246.
17 Errico F, Nistico R, Napolitano F, Oliva AB, Romano R, Barbieri F *et al.* Persistent increase of D-aspartate in D-aspartate oxidase mutant mice induces a precocious hippocampal age-dependent synaptic plasticity and spatial memory decay. *Neurobiol Aging* 2011; **32**: 2061–2074.
18 Errico F, Rossi S, Napolitano F, Catuogno V, Topo E, Fisone G *et al.* D-aspartate prevents corticostriatal long-term depression and attenuates schizophrenia-like symptoms induced by amphetamine and MK-801. *J Neurosci* 2008; **28**: 10404–10414.
19 Kim PM, Duan X, Huang AS, Liu CY, Ming GL, Song H *et al.* Aspartate racemase, generating neuronal D-aspartate, regulates adult neurogenesis. *Proc Natl Acad Sci USA* 2010; **107**: 3175–3179.
20 Errico F, Napolitano F, Squillace M, Vitucci D, Blasi G, de Bartolomeis A *et al.* Decreased levels of d-aspartate and NMDA in the prefrontal cortex and striatum of patients with schizophrenia. *J Psychiatr Res* 2013; **47**: 1432–1437.
21 Coyle JT. NMDA Receptor and Schizophrenia: A Brief History. *Schizophr Bull* 2012; **38**: 920–926.
22 Moghaddam B, Javitt D. From revolution to evolution: the glutamate hypothesis of schizophrenia and its implication for treatment. *Neuropsychopharmacology* 2012; **37**: 4–15.
23 Errico F, Pirro MT, Affuso A, Spinelli P, De Felice M, D'Aniello A *et al.* A physiological mechanism to regulate D-aspartic acid and NMDA levels in mammals revealed by D-aspartate oxidase deficient mice. *Gene* 2006; **374**: 50–57.
24 Nistico R, Mango D, Mandolesi G, Piccinin S, Berretta N, Pignatelli M *et al.* Inflammation subverts hippocampal synaptic plasticity in experimental multiple sclerosis. *PLoS One* 2013; **8**: e54666.
25 Rompala GR, Zsiros V, Zhang S, Kolata SM, Nakazawa K. Contribution of NMDA receptor hypofunction in prefrontal and cortical excitatory neurons to schizophrenia-like phenotypes. *PLoS One* 2013; **8**: e61278.
26 Ferrari L, Turrini G, Crestan V, Bertani S, Cristofori P, Bifone A *et al.* A robust experimental protocol for pharmacological fMRI in rats and mice. *J Neurosci Methods* 2012; **204**: 9–18.
27 Gozzi A, Jain A, Giovannelli A, Bertollini C, Crestan V, Schwarz AJ *et al.* A neural switch for active and passive fear. *Neuron* 2010; **67**: 656–666.
28 Sforazzini F, Schwarz AJ, Galbusera A, Bifone A, Gozzi A. Distributed BOLD and CBV-weighted resting-state networks in the mouse brain. *Neuroimage* 2014; **87**: 403–415.
29 Dodero L, Damiano M, Galbusera A, Bifone A, Tsaftsaris SA, Scattoni ML *et al.* Neuroimaging evidence of major morpho-anatomical and functional abnormalities in the BTBR T+TF/J mouse model of autism. *PLoS ONE* 2013; **8**: e76655.
30 Gozzi A, Tessari M, Dacome L, Agosta F, Lepore S, Lanzoni A *et al.* Neuroimaging evidence of altered fronto-cortical and striatal function after prolonged cocaine self-administration in the rat. *Neuropsychopharmacology* 2011; **36**: 2431–2440.
31 Mandeville JB, Marota JJ, Kosofsky BE, Keltner JR, Weissleder R, Rosen BR *et al.* Dynamic functional imaging of relative cerebral blood volume during rat forepaw stimulation. *Magn Reson Med* 1998; **39**: 615–624.
32 Schwarz AJ, Reese T, Gozzi A, Bifone A. Functional MRI using intravascular contrast agents: detrending of the relative cerebrovascular (rCBV) time course. *Magn Reson Imaging* 2003; **21**: 1191–1200.
33 Gozzi A, Agosta F, Massi M, Ciccocioppo R, Bifone A. Reduced limbic metabolism and fronto-cortical volume in rats vulnerable to alcohol addiction. *Neuroimage* 2013; **69**: 112–119.
34 Smith SM, Jenkinson M, Woolrich MW, Beckmann CF, Behrens TE, Johansen-Berg H *et al.* Advances in functional and structural MR image analysis and implementation as FSL. *Neuroimage* 2004; **23 Suppl 1**: S208–S219.
35 D'Amelio M, Cavallucci V, Middei S, Marchetti C, Pacioni S, Ferri A *et al.* Caspase-3 triggers early synaptic dysfunction in a mouse model of Alzheimer's disease. *Nat Neurosci* 2011; **14**: 69–76.
36 Colantuoni C, Lipska BK, Ye T, Hyde TM, Tao R, Leek JT *et al.* Temporal dynamics and genetic control of transcription in the human prefrontal cortex. *Nature* 2011; **478**: 519–523.
37 Colantuoni C, Henry G, Zeger S, Pevsner J. SNOMAD (Standardization and NOrmalization of MicroArray Data): web-accessible gene expression data analysis. *Bioinformatics* 2002; **18**: 1540–1541.
38 Leek JT, Storey JD. Capturing heterogeneity in gene expression studies by surrogate variable analysis. *PLoS Genet* 2007; **3**: 1724–1735.
39 Martino D, Di Giorgio A, D'Ambrosio E, Popolizio T, Macerollo A, Livrea P *et al.* Cortical gray matter changes in primary blepharospasm: a voxel-based morphometry study. *Mov Disord* 2011; **26**: 1907–1912.
40 Bertolino A, Caforio G, Blasi G, De Candia M, Latorre V, Petruzzella V *et al.* Interaction of COMT (Val(108/158)Met) genotype and olanzapine treatment on prefrontal cortical function in patients with schizophrenia. *Am J Psychiatry* 2004; **161**: 1798–1805.
41 Errico F, Napolitano F, Nistico R, Usiello A. New insights on the role of free D: -aspartate in the mammalian brain. *Amino Acids* 2012; **43**: 1861–1871.
42 Schobel SA, Chaudhury NH, Khan UA, Paniagua B, Styner MA, Asllani I *et al.* Imaging patients with psychosis and a mouse model establishes a spreading pattern of hippocampal dysfunction and implicates glutamate as a driver. *Neuron* 2013; **78**: 81–93.
43 Matsuzaki M, Honkura N, Ellis-Davies GC, Kasai H. Structural basis of long-term potentiation in single dendritic spines. *Nature* 2004; **429**: 761–766.
44 Okamoto K, Nagai T, Miyawaki A, Hayashi Y. Rapid and persistent modulation of actin dynamics regulates postsynaptic reorganization underlying bidirectional plasticity. *Nat Neurosci* 2004; **7**: 1104–1112.
45 Tang SJ, Reis G, Kang H, Gingras AC, Sonenberg N, Schuman EM. A rapamycin-sensitive signaling pathway contributes to long-term synaptic plasticity in the hippocampus. *Proc Natl Acad Sci USA* 2002; **99**: 467–472.
46 Costa-Mattioli M, Sossin WS, Klann E, Sonenberg N. Translational control of long-lasting synaptic plasticity and memory. *Neuron* 2009; **61**: 10–26.
47 Huang W, Zhu PJ, Zhang S, Zhou H, Stoica L, Galiano M *et al.* mTORC2 controls actin polymerization required for consolidation of long-term memory. *Nat Neurosci* 2013; **16**: 441–448.
48 Engert F, Bonhoeffer T. Dendritic spine changes associated with hippocampal long-term synaptic plasticity. *Nature* 1999; **399**: 66–70.

49 Maletic-Savatic M, Malinow R, Svoboda K. Rapid dendritic morphogenesis in CA1 hippocampal dendrites induced by synaptic activity. *Science* 1999; **283**: 1923–1927.
50 Gong LQ, He LJ, Dong ZY, Lu XH, Poo MM, Zhang XH. Postinduction requirement of NMDA receptor activation for late-phase long-term potentiation of developing retinotectal synapses in vivo. *J Neurosci* 2011; **31**: 3328–3335.
51 Huang YY, Nguyen PV, Abel T, Kandel ER. Long-lasting forms of synaptic potentiation in the mammalian hippocampus. *Learn Mem* 1996; **3**: 74–85.
52 Lamprecht R, LeDoux J. Structural plasticity and memory. *Nat Rev Neurosci* 2004; **5**: 45–54.
53 Wang SH, Morris RG. Hippocampal-neocortical interactions in memory formation, consolidation, and reconsolidation. *Annu Rev Psychol* 2010; **61**: 49–79, C1-4.
54 Javitt DC. Twenty-five years of glutamate in schizophrenia: are we there yet? *Schizophr Bull* 2012; **38**: 911–913.
55 Sawa A, Snyder SH. Schizophrenia: neural mechanisms for novel therapies. *Mol Med* 2003; **9**: 3–9.
56 Bertolino A, Blasi G. The genetics of schizophrenia. *Neuroscience* 2009; **164**: 288–299.

Supplementary Information accompanies the paper on the Translational Psychiatry website (http://www.nature.com/tp)